Laser Spectroscopy

James Amarel and Dr. Matt Moelter

June 16, 2017

1 Goal

To investigate Doppler broadening of a Rubidium vapor with single laser spectroscopy and then use a two laser apparatus to perform the saturated-absorption technique for Doppler-free measurements of Rubidium's hyperfine structure.

2 Introduction/Background

A laser beam traversing an atomic vapor sample is attenuated when in resonance with an atomic transition. For a monochromatic laser, the absorption is greatest at resonance frequency f_o, which is measured as an absorption dip with linewidth Δf. For low density samples, the resonance frequency is broadened due to the thermal motion of the atoms, which allows for off resonance photons to be Droppler shifted into resonance, broadening the range of absorbable frequencies. The velocity distribution of gaseous molecules, as determined by Boltzmann statistics, leads to a Gaussian expression for the Doppler lineshape of a spectral line

$$S(f) = Ce^{-4\ln 2(f-f_o)^2/(\Delta f)^2} \tag{1}$$

where the Doppler width is

$$\Delta f = \sqrt{\frac{8\ln 2kT}{mc^2}} f_o \tag{2}$$

and m is the atomic mass. In practice, multiple spectral lines are present due to the atomic velocity distribution, which, when separated by less than the Doppler width, will blend into an unresolved spectral line of greater width. Upon being stimulated into an excited state, the atoms rapidly decay (within nanoseconds) to ground. While a strong laser can momentarily overcome spontaneous emission by trapping atoms in their excited states, stimulated emission quickly moves the system to a transition saturated state.

A saturated-absorption signal can be obtained by splitting a laser beam into two beams of different intensity, and then overlapping them, in crossed directions, within a vapor cell. In the saturated-absorption technique, the beams are restricted to interacting with atoms that have zero velocity along the beam direction, which results in a Doppler-free measurement. If the laser is tuned to a frequency that is off resonance, the crossed beams will interact with two disjoint sets of atoms, since the photons must be Doppler shifted onto resonance and the necessary atomic velocity will be different for each laser. In contrast, when the laser is tuned to resonance, the beams are competing to excite atoms with a velocity component of zero perpendicular to the beam, now the beams are competing within same set. Therefore, if the strong beam (pump beam) is capable of saturating the transition, there are significantly less

atoms available to absorb photons of the weak beam (probe beam); this provides a measurable response with resolution unobstructed by Doppler broadening.

In this experiment, we use a dilute gas of rubidium atoms, containing approximately 70% ^{85}Rb, which carries $I = 5/2$, and 30% ^{87}Rb, which carries $I = 3/2$, and are Hydrogen-like with a single valence electron in $n = 5$ above a closed $n = 4$ shell. Due to valence electron-spin orbit coupling, more energy is required for $\vec{L}$ and $\vec{S}$ to be aligned, than for the two to be anti-aligned, where $\vec{L}$ is the electron's orbital angular momentum and $\vec{S}$ is the electron's intrinsic angular momentum. Since our laser was of wavelength 780 nm, we investigated the $5S_{1/2} \leftrightarrow 5P_{3/2}$ transition. Note that with hyperfine splitting, the $5S_{1/2}$ ($5P_{3/2}$) state of ^{85}Rb has available states $F = 2, 3$ ($F = 1, 2, 3, 4$) and, in ^{87}Rb, the $5S_{1/2}$ ($5P_{3/2}$) state may be $F = 1, 2$ ($F = 0, 1, 2, 3$).

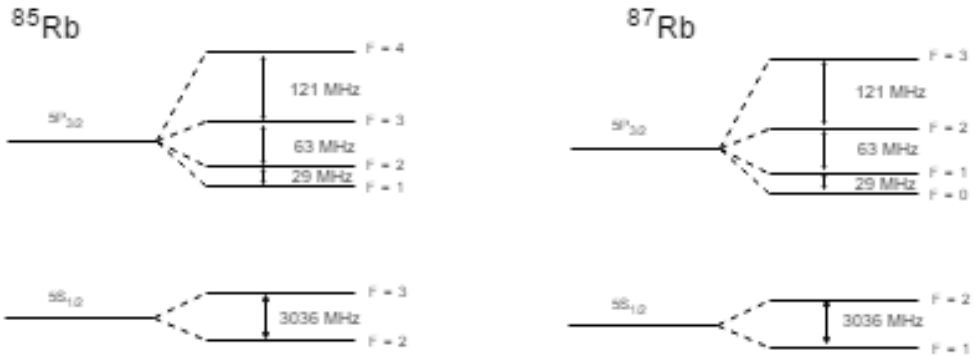

Figure 1: Energy level transitions for both Rubidium isotopes.

Hyperfine splitting is the result of electron-nuclear coupling and $F = J + I$ is the total atomic angular momentum. Since the energy associated with the $5S_{1/2} \leftrightarrow 5P_{3/2}$ transition is equivalent for both ^{85}Rb and ^{87}Rb when only considering their fine structure, it is necessary to resolve the hyperfine structure in order to distinguish the two isotopes. At hyperfine resolution, there are six normal (meaning $\Delta F = 0, \pm 1$) $5S_{1/2} \leftrightarrow 5P_{3/2}$ transitions for each isotope, three from each of the F degenerate $5S_{1/2}$ levels, which are separated by width 6835 MHz (larger than Doppler broadening) and terminate in the $5P_{3/2}$ state with spacing ~ 100 MHz (less than the Doppler width). We shall denote the transition lines from the lower energy $F = 1$ ($F = 2$) $5S_{1/2}$ state as 87a (85a) and those originating with $F = 2$ ($F = 3$) as 87b (85b). Thus, one may expect that the Doppler-free absorption spectrum should contain three narrow peaks for each transition line, but this is not true in the presence of cross-over resonance, which occurs when there are two atomic states f_1 and f_2 with separation less than the Doppler width. In this case, a saturation-absorption signal occurs at frequency $(f_1 + f_2)/2$ due to atoms of precise velocity such that, f_1 is blue shifted into pump beam resonance and f_2 is red shifted (due to crossing) into probe beam resonance. Note that, while $\Delta F = +1$ transitions tend to be stronger than their $\Delta F = 0, -1$ counterparts, cross-over resonances in a saturated-absorption spectrum typically dominate over the normal transitions.

3 Procedure and Data

First, we used a single beam technique to measure the absorption spectrum of isotopes Rubidium-87 and Rubidium-85 using a tunable diode laser and photodiode, with the setup shown in Figure 2. Before entering the camera recorded Rubidium chamber, the laser beam passed through a neutral density filter, to shield the sensitive photodiode, and is redirected by a beam splitter prior to being collimated by an iris of approximately 1 cm width. The

photodiode measures the absorption dip when on resonance and the TV camera allows for visual confirmation of when the beam is on resonance.

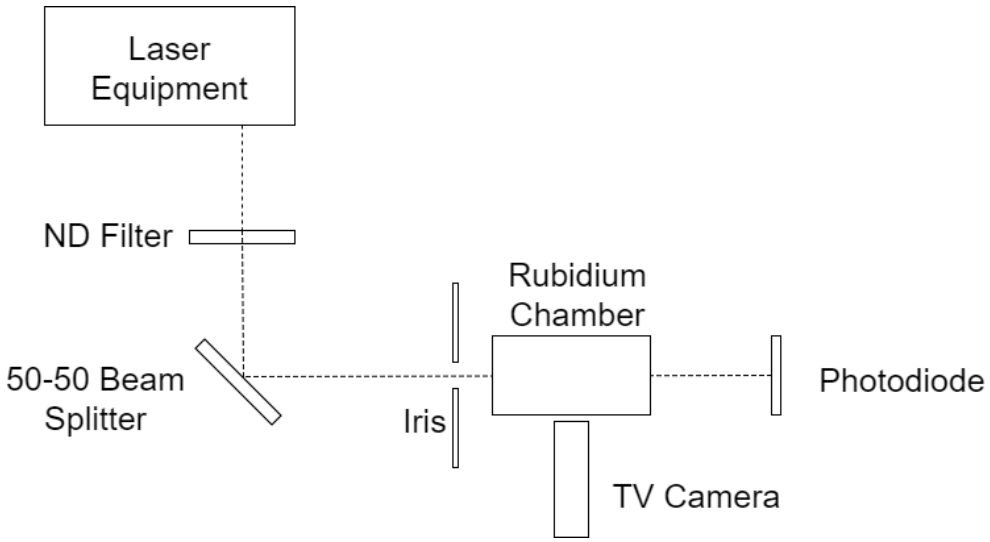

Figure 2: Experimental setup for single beam spectroscopy.

The laser frequency scans back and forth within the range set by a built in cavity which is adjusted in length according the drive signal of its piezoelectric motor and crosses resonance at a rate of twenty times per second, causing the sample to fluoresce. In order to reduce the presence of mode hops, which is when the laser frequency doesn't vary smoothly due to a significant change in cavity length and causes discontinuous signal jumps, we modulated the laser current simultaneously with the piezo scan. This changes the temperature of the diode laser's p-n junction, which affects the average atomic separation and shifts the lattice supported standing wave modes, allowing for long scans with range $\sim 20\ GHz$ without mode hops.

Then, we used an oscilloscope to measure the Doppler broadened absorption lines of our Rubidium vapor, which is shown in Figure 3 and should be viewed as a signal with a sloped baseline, which is due to the cavity frequency response curve, and can be overcome to obtain the true signal by sending a portion of the laser beam, before it passes through the Rubidium cell, into a secondary photodiode and performing a baseline subtraction between the two signals, as seen in Figure 4.

In order to measure the hyperfine splitting in the spectrum of both Rubidium isotopes, we converted the horizontal time axis of Figure 4 into the frequency scale by referencing the image shown in Figure 5, which shows the Faby-Perot interferometer fringes for a laser that is scanning across the absorption spectrum of Rubidium vapor. Since there are 13.6 fringes between the 87b and 87a absorption lines, the laser satisfied the condition for standing waves within the interferometer 13.6 times, from which we can use the standing wave condition within a closed cavity of length to find the overall change in laser frequency

$$\Delta f = \frac{c}{2L}\Delta n = 6.79 \text{ GHz} \tag{3}$$

where $L = 30\ cm$ is the Faby-Perot cavity length, c is the speed of light, and $\Delta n = 13.6$.

Equation 3, in combination with an oscilloscope measurement of the time difference $\Delta t = 22.0 \pm 1.7\ ms$ between the 87b and 87a absorption lines provides the calibration relation $\frac{\Delta t}{\Delta f} = 307$ MHz per ms, which we used to determine the frequency separations between the four peaks, as seen in Table 1.

Additionally, we determined the FWHM of each absorption line by performing a Gaussian fit to the individual dips in Figure 4, which is shown in Table 2. All four peaks have a FWHM

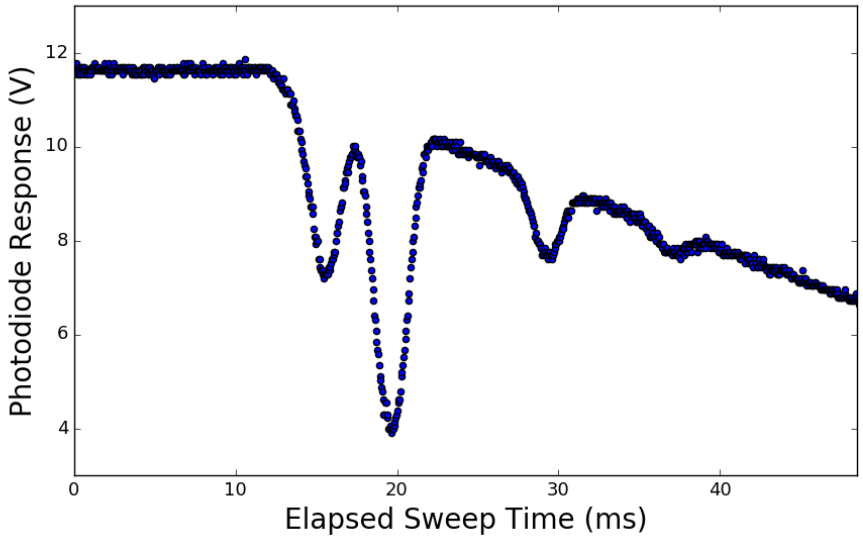

Figure 3: Oscilloscope readout of the Rubidium absorption spectrum (lower), displaying dips from left to right in order 87b, 85b, 85a, and 87a. The upper signal is the drive ramp for the piezo.

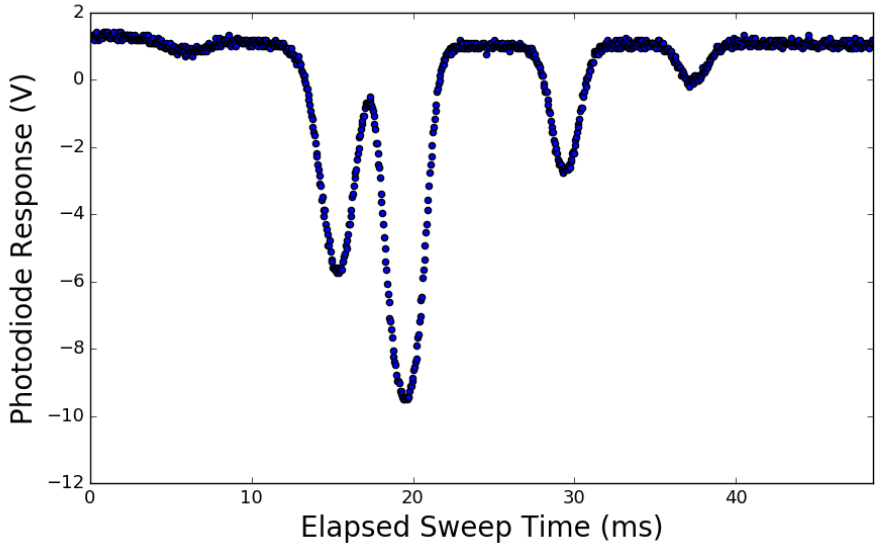

Figure 4: Baseline subtraction of the Rubidium absorption spectrum.

Table 1: Time and frequency separation between the four absorption peaks.

	87b-87a	87b-85b	85b-85a	85a-87a
Δt (ms)	22.0 ± 1.7	4.2 ± 0.5	9.9 ± 0.9	7.9 ± 1.9
Δf (MHz)	6750 ± 40	1300 ± 150	3000 ± 300	2400 ± 500

on order 1000 MHz, which is much larger than what should be expected for a laser of line width 500 KHz and is due to the Doppler broadening of the absorption line.

To obtain a Doppler free signal, we used a two laser setup, as seen in Figure 6, to select one velocity group, which allowed us to resolve the 87b line at hyperfine resolution. Two resonance beams were deflected by a 90:10 beam splitter before traveling through a rubidium chamber such that the pump beam saturated the transition so that the probe beam provides a

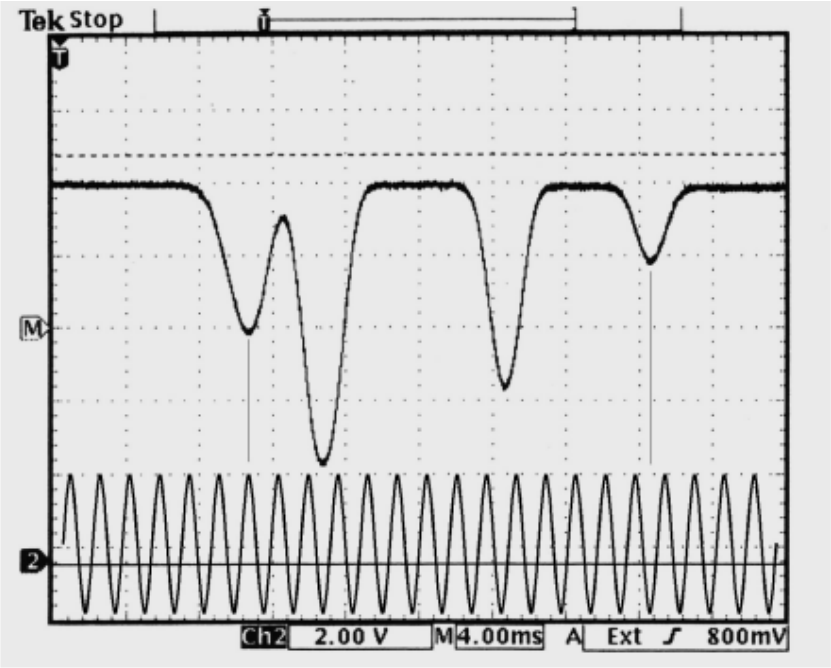

Figure 14: An absorption spectrum with baseline subtraction. The lower trace shows the fringes from a Fabry-Perot interferometer.

Figure 5: .

Table 2: Full width at half max of the absorption peaks in time and frequency scale.

	87b	85b	85a	87a
FWHM (ms)	3.16 ± 0.02	2.62 ± 0.02	1.62 ± 0.02	8.6 ± 0.2
FWHW (MHz)	970 ± 6	804 ± 6	497 ± 6	2640 ± 60

saturated-absorption signal where there is a spike in photodiode response when on resonance, since the beams are in competition within the same set.

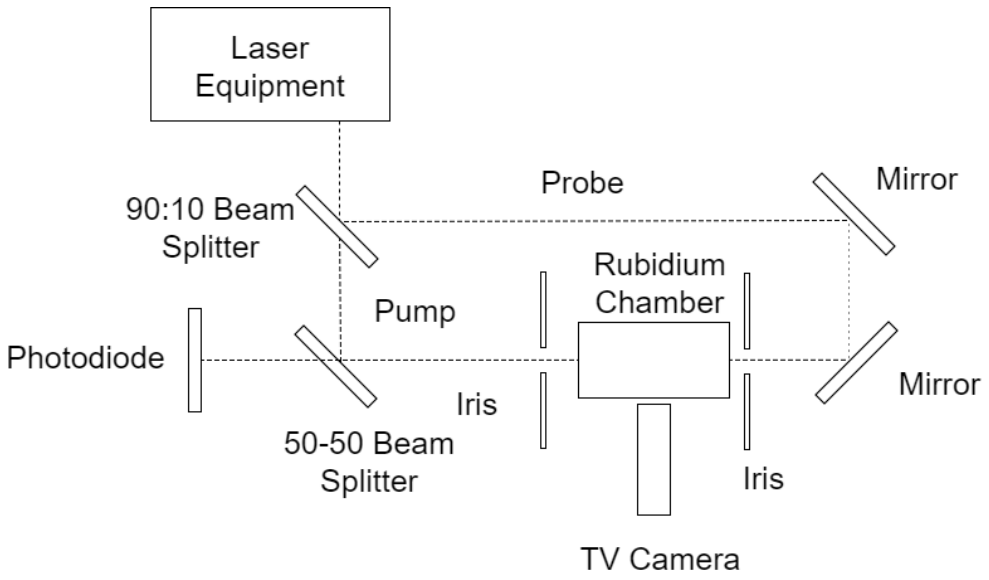

Figure 6: Experimental setup for two beam, Doppler-free spectroscopy.

We then repeated the procedure of our single laser measurements, including baseline subtraction, to measure Rubidium's hyperfine spectrum, which is shown in Figure 7. Figure

8 is the enhanced 87b line (the left dip) was expected to contain a faint saturated absorption signal near its minimum corresponding to the $F = 2 \rightarrow 3$ transition, which is the strongest of the normal transitions.

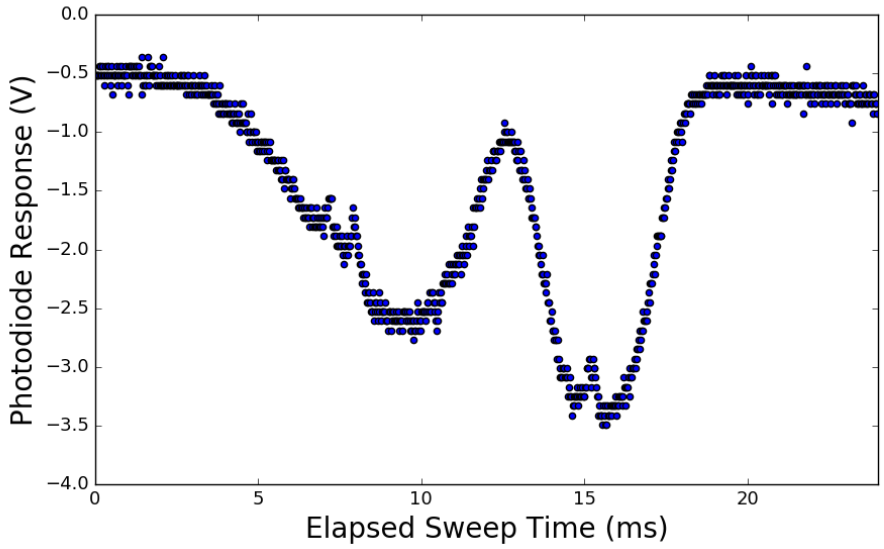

Figure 7: Hyperfine spectrum of Rubidiums 87b and 85b lines, as measured with the saturated-absorption technique.

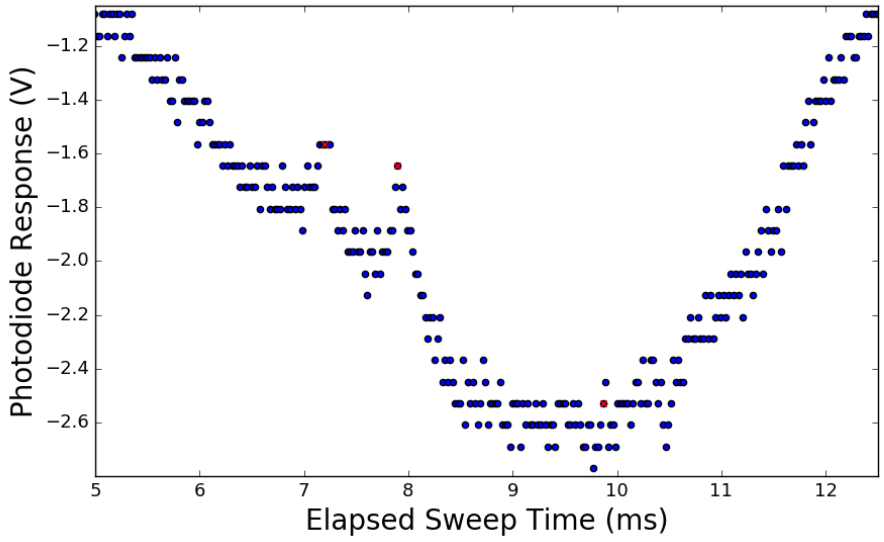

Figure 8: Hyperfine spectrum of Rubidiums 87b.

It is not immediately obvious if an absorption line for the $F = 2 \rightarrow 3$ transition is present in our hyperfine Rubidium spectrum, although it does contain peaks located at the C 1-3 and C 2-3 cross-over resonances, so we shall proceed under the assumption that the $F = 2 \rightarrow 3$ transition is the faint peak at $t_{F_{23}} = 9.88 \pm 0.04$ ms, which is marked in Figure 8, along with the two cross over peaks, which appear at times $t_{C_{13}} = 7.20 \pm 0.05$ ms and $t_{C_{13}} = 7.90 \pm 0.05$ ms. Table 3 contains our measurements for the transition frequency of between the $F = 2 \rightarrow 3$, C 1-3, and C 2-3 transition lines, which we obtained via a calibration with our previously measured value for FWHM of the 87b line. Cross-over resonances occur when

multiple transitions that share a common ground state are available to the same Doppler-broadened beam, creating a crossover peak at the average transition energy and is due to atom motion causing the pump and probe beams to be on resonance with two separate transitions. In this case, the pump beam depopulates the ground state and saturates one transition, then the probe beam finds fewer atoms in the ground state and its absorption falls.

Table 3: Time and frequency separation between the hyperfine $F = 2 \rightarrow 3$, C 1-3, and C 2-3 transition lines.

	C13-F23	C23-C13
Δt (ms)	1.92 ± 0.05	0.70 ± 0.05
Δf (MHz)	418 ± 10	152 ± 10

Our calibration relation converted and scaled the temporal separation of the peaks in Figure 8 by taking the ratio of the FWHM of the hyperfine spectrum to the lower resolution spectrum. Additionally, we determined the FWHM of the two cross-over resonances, which is shown in Table 4, where both transitions share the same FWHM, since the measurements are taken with the same set of atoms.

Table 4: FWHM of two 87b cross-over resonance lines in the hyperfine Rubidium spectrum.

	C-23	C-13
FWHM (MHz)	50 ± 15	50 ± 15

Notice that the linewidth Doppler shifted signal (our first measurement) has an uncertainty on order of the FWHM of the peaks of our hyperfine crossover measurements. This is due to the fact that the Doppler width for 780 nm laser and Rubidium vapor at 50^oC, as determined by Equation 1, is $\Delta f_{Dop} = 535$ MHz. A typical spectrometer has an instrumental linewidth of ~ 0.005 nm, corresponding to a resolution of 6.41×10^{-6}, and is incapable of resolving Doppler broadening, which requires resolution on order $\Delta f_{Dop}/f_{signal} = 1.39 \times 10^{-6}$. The laser in our experiment has $\Delta f_{laser} = 500$ KHz, which provides resolution on order of 10^{-9} and has no difficulty resolving Doppler profiles.

4 Analysis and Discussion

Since the hyperfine splitting in the final states is negigible compared to the difference in energy between the 87b and 87a (85b and 85a), the entries in Table 1 provide hyperfine splitting measurements of 6750 ± 40 MHz for 87b-87a and 3000 ± 300 MHz for 85b-85a. These results are in great agreement with the known frequency separation between 87b-87a and 85b-85a of 6835 MHz and 3036 MHz, respectively, although both measurements show the transition energies are lower than as predicted by the hydrogen-like approximation for Rubidium. This may indicate that the outermost electrons are shielded from the nuclear charge and as consequence, their states are of lower energy than the model predicts.

Inverting Equation 1 provides the relationship

$$T = (\frac{\Delta f}{f})^2 \frac{mc^2}{8 \ln 2 k 6} \tag{4}$$

between the temperature and signal broadening, which, for $\Delta f \sim FWHM$, where we use the FWHM values from Table 2, yields measurements of the sample temperature, as shown in Table 5 below,

Since our experiment was performed at 323 K, it is evident that Doppler broadening is not the only culprit in enlarging the linewidth, another likely broadening source is due to

Table 5: Predicted temperature values of the Rubidium cell under the assumption that the Doppler effect is the only broadening source.

Absorption Line	Temperature ±13 (K)
87b	1061
85b	729
85a	278

the collision of the gas particles, which interrupts emission processes, increasing the lifetime uncertainty and broadening the energy spectrum.

From our hyperfine measurements of the cross-over transitions, we estimate the lifetime of Rubidium's 5p states from the Heisenberg uncertainty principle $\Delta t = \hbar/2\Delta E = \hbar/2h\Delta f = 1.6 \pm 0.5$ ns, which is of reasonable order for an atomic transition.

We also determine the transition frequency for $F = 1 \rightarrow 3$ by noting that, since crossover transitions occur at the average frequency between two transitions from

$$f_{C23} - f_{C13} = \frac{1}{2}(f_3 + f_2) - \frac{1}{2}(f_3 + f_1) = \frac{1}{2}(f_2 - f_1) \tag{5}$$

which provides $f_{21} = 300 \pm 20$ MHz and, similarly, we found $f_{23} = 530 \pm 20$ MHz, both of which are twice that of the accepted transition frequencies of 157 MHz and 267 MHz, respectively.

5 Conclusion

In total, we measured the Doppler broadened peaks of the Rubidium spectrum using single laser spectroscopy and determined the hyperfine splitting between the 87a-87b and 85a-85b transitions as 6750 ± 40 MHz and 3000 ± 300 MHz, respectively, which was in agreement with the accepted values of 6835 MHz and 3036 MHz, respectively. We were also able to infer that Doppler broadening is not the only broadening source in our system from the fact that the FWHM of our absorption dips was significantly greater than the predicted Doppler broadening.

Then we utilized the saturated-absorption technique to obtain a Doppler-free signal and measure the hyperfine line widths of the $F = 2 \rightarrow 3$, C-13, and C-23 transitions, which allowed us to use the uncertainty principle to make a reasonable estimate the lifetime of Rubidium's 5p state to be 1.9 ± 0.5 ns. And finally, we used our measurements of the frequency separation between the hyperfine states to determine the hyperfine structure of Rubidium for the $F = 1 \rightarrow 2$ and $F = 2 \rightarrow 3$ transitions, where we found $f_{23} = 530 \pm 20$ MHz and $f_{13} = 300 \pm 20$ MHz.